BULLETIN OF THE POLISH ACADEMY OF SCIENCES
TECHNICAL SCIENCES, Vol. 71(3), 2023, Article number: e144619
DOI: 10.24425/bpasts.2023.144619

The optimization of the TMDI for efficient mitigation of the vibration

Konrad MNICH and Przemyslaw PERLIKOWSKI*

Division of Dynamics, Lodz University of Technology, Stefanowskiego 1/15, 90-924 Lodz, Poland

Abstract. The paper concerns the optimization of a tuned mass damper with inerter (TMDI) based on two strategies, i.e., the minimum amplitude in the resonance peak and minimum area under the frequency response curve. The optimization is based on real, accessible parameters. Both optimization procedures are presented in two steps. In the first one, two parameters of the TMDI are tuned (inertance and damping coefficient), while in the second one, three parameters (mass, inertance, and damping coefficient). We show that both strategies give the optimum sets of parameters and allow the reduction of the amplitude of the damped system.

Key words: tuned mass damper; inerter; optimization; mitigation of vibrations.

1. INTRODUCTION

In this paper, we demonstrate a numerical optimization method of a tuned mass damper with an inerter (TMDI). It is a continuation of research work on increasing the efficiency of the TMDI. The ordinary tuned mass damper (TMD) biggest shortcoming is its narrow range of operation, limited to the single frequency value and its close vicinity. The problem can be overcome by making the device semi-active so that its parameters are adjusted according to the conditions. Many research teams have demonstrated that such live adjustments would improve the damping performance of the device [1–4].

Based on these discoveries, one can formulate two engineering questions to be answered in the process: how to vary the parameters of the actual device and what optimization criteria to choose for the parameters adjustment. Given that a regular TMD consists of a mass, a spring, and a damper, one must be able to modify at least one of them to move the resonance peaks of the protected construction to the safe regions. An improvement proposed by Brzeski *et al.* in 2015 [5] consisted of adding to the system an inerter with variable inertance, which had a similar effect to having an adjustable mass.

The idea was further developed, and the working prototypes were built, proving the concept [6]. In parallel, a research team led by Yinlong Hu developed a similar idea with a different hardware implementation [7]. Adding the inertance to the TMD was a workaround to vary the device inertial properties reliably and easily, but the variation of the mass itself was also proved possible. For example, Weixing Shi *et al*. demonstrated a TMD in which the mass could be changed thanks to the water flowing in and out [8, 9]. Others exploited the variable stiffness of the suspension as a way to change the dynamic behavior of the damper [10–12].

Finally, viscous damping can be varied too, and two main approaches make it possible. Dashpots filled with the magnetorheological fluid can vary their damping as a function of the magnetic field applied [13]. Alternatively, one can throttle the flow of the damping fluid, which also affects the overall damping coefficient. Both approaches were investigated and tested in the context of TMDs [11, 14–16].

Knowing that the live control of all the parameters of the TMD is impossible, one must choose the right criterion for their optimization. From a global perspective, one common approach is to minimize the height of the resonance peaks of the damped construction, as demonstrated by Den Hartog a long time ago [17]. Alternatively, one can be interested in minimizing the average amplitude response within a given range of excitation [18, 19]. Other aspects that must be considered in the tuning process are the mass ratio of the TMD and the damped mass [20,21], and in the case of TMDI, the ratio of the inertance to the real tuned mass [22–24].

Within this context, after the successful development of a TMDI, a TMDI with variable damping became the next target of our research team. The first step was a series of simulations published in 2020 to demonstrate that changing the damping can improve the performance of the TMD [25]. This study was purely numerical, and in the next step, a model of a real dashpot with a variable damping coefficient had to be created. Although the dashpots with variable damping became a common thing in the industry, the characteristics of the off-the-shelf parts are not made public by the manufacturers and a specifically designed experiment had to be conducted to get a reliable model of the dashpot. The paper published by Mnich *et al*. in 2020 details the procedure used to build a numerical model of the real dashpot in the form of a polynomial surface [16]. The creation of a reliable model of the dashpot was necessary since the goal of the research is to confirm the simulations experimentally. The reasoning described so far led to the study presented in this paper. With the knowledge that variable damping can improve the performance of the TMDI and with the model of a real dashpot

*e-mail: przemyslaw.perlikowski@p.lodz.pl

Manuscript submitted 2022-10-23, revised 2022-12-29, initially accepted for publication 2023-01-16, published in June 2023.

with variable damping, the authors propose a method of optimization of the parameters in a TMDI employing two criteria.

The paper is organized as follows. In Section 2, we show the model of the system. Then, in Section 3, the methodology of the optimization is proposed. Section 4 includes the results of two optimization approaches. Finally, we conclude our findings in the last section.

2. MODEL OF SYSTEM WITH TMDI

The model of the system is presented in Fig. 1. We show it in two levels of detail. In panel (a), the physical model is presented. It consists of the main system with mass M, fixed to the ground by spring with stiffness $6K$, and a dashpot with damping coefficient C. It is enforced with kinematic harmonic excitation with amplitude A and frequency ω. The main system is damped-out with the TMDI with mass m. The systems are coupled with spring with stiffness k and dashpot with damping coefficient c. The systems also interact with the inerter. The rack is a part of the TMDI, while the pinion with the pitch radius r_p oscillates with the main mass. The pinion is interconnected with the flywheel, and their complete moment of inertia is given by I. Thus, the mass of the pinion and flywheel is added to the main mass. Such a solution enables us to design less massive TMDI than the classical TMD with the same damping efficiency. The schematic model of the system is shown in panel (b). Now, we see the inerter with inertance $I_{\text{iner}} = \dfrac{I}{r_p^2}$. For simplicity in the future study, we will use just I_{iner} and neglect the change of mass M due to the change of mass of the flywheel. Equations of system motion are given as follows:

$$M\ddot{x} + 7Kx + C\dot{x} + k(x-y) + c(\dot{x}-\dot{y}) + I_{\text{Iner}}(\ddot{x}-\ddot{y}) = KA\cos(\omega t), \tag{1}$$

$$m\ddot{y} - k(x-y) - c(\dot{x}-\dot{y}) - I_{\text{Iner}}(\ddot{x}-\ddot{y}) = 0, \tag{2}$$

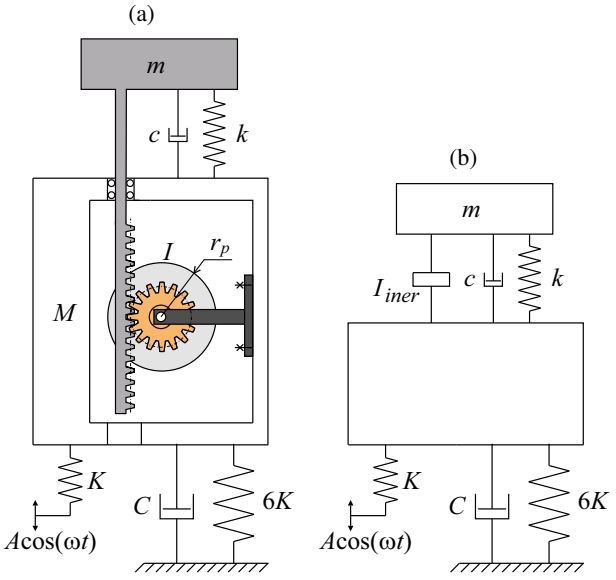

Fig. 1. Model of the system in two levels of details: (a) physical model; (b) schematic model

where:

$M = 102.66$ kg, $K = 8181.0$ N/m, $C = 2.0\xi_1\sqrt{7MK}$ Ns/m, $\xi_1 = 0.01$, $k = 10448$ N/m, $c = 2.0\xi_2\sqrt{mk}$ Ns/m, $A = 0.03$ m and ω, m, ξ_2, I_{iner}, are controlling parameters. The values of parameters correspond to real values taken from our experimental rig studied in previous paper [6]. In laboratory implementation the mass of the TMDI was $m = 11.26$ kg. The intertance was variable, while in this study we use a fixed value.

We solve equations (1, 2) analytically. We assume the following forms of solutions: $x = a_1\cos(\omega t) + b_1\sin(\omega t)$ and $y = c_1\cos(\omega t) + d_1\sin(\omega t)$ and we substitute them to equations of motion. We get following solutions:

$$\begin{aligned}
a_1 &= AK\left(c^2\omega^2(7K-\omega^2 Q) - 14kK\omega^2(I_{\text{Iner}}+m)\right.\\
&\quad + k\omega^4(2I_{\text{Iner}}Q + m(m+2M)) + \omega^4(I_{\text{Iner}}+m)\big(7K(I_{\text{Iner}}+m)\\
&\quad \left.-\omega^2(M(I_{\text{Iner}}+m)+I_{\text{Iner}}m)\big) + k^2(7K-\omega^2 Q)\right)/H,\\
b_1 &= AK\omega\left(C\left(c^2\omega^2 + (k-\omega^2(I_{\text{Iner}}+m))^2\right) + cm^2\omega^4\right)/H,\\
c_1 &= AK\left(\omega^4(-c(Cm+cQ) + kM(2I_{\text{Iner}}+m) + 2I_{\text{Iner}}km\right.\\
&\quad + 7I_{\text{Iner}}K(I_{\text{Iner}}+m)) + \omega^2(7c^2K - k(7K(2I_{\text{Iner}}+m)+kQ))\\
&\quad \left.-I_{\text{Iner}}\omega^6(I_{\text{Iner}}Q+mM) + 7k^2K\right)/H,\\
d_1 &= AK\omega\left(\omega^2\left(C(c^2 - k(2I_{\text{Iner}}+m)) + 7cKm\right)\right.\\
&\quad \left.+\omega^4(CI_{\text{Iner}}(I_{\text{Iner}}+m) - cmM) + Ck^2\right)/H,
\end{aligned}$$

and denominator is equal to:

$$\begin{aligned}
H &= c^2\omega^2(C^2\omega^2 + (\omega^2 Q - 7K)^2) + \omega^6(I_{\text{Iner}}+m)(C^2(I_{\text{Iner}}+m)\\
&\quad - 14K(I_{\text{Iner}}Q + mM)) + 2k\omega^2(\omega^2(7K(2I_{\text{Iner}}Q + m(m+2M))\\
&\quad - C^2(I_{\text{Iner}}+m)) - 49K^2G - \omega^4 Q(I_{\text{Iner}}Q + mM))\\
&\quad + k1^2(C^2\omega^2 + (\omega^2 Q - 7K)^2) + 2Ccm^2\omega^6\\
&\quad + 49K^2\omega^4(I_{\text{Iner}}+m)^2 + \omega^8(I_{\text{Iner}}Q + mM)^2,
\end{aligned}$$

where $Q = (M+m)$. Formula corresponding to amplitude of the main body is given by $\text{Amp}_x(\omega, I_{\text{Iner}}, \xi_2, m) = \sqrt{a_1^2 + b_1^2}$. Based on this formula we are able to calculate the time response as well as the FRC (frequency response curve).

3. METHODS

In this section, we present the methodology of optimization. We assume that parameters of main mass (M, K, ξ_1), stiffness of spring k between main mass and TMDI, and amplitude of forcing A are fixed. Based on the preliminary study we can assume that the frequency of the excitation ω is varying in range $\omega \in [\omega(\min), \omega(\max)]$, where $\omega(\min) = 5$ rad/s and $\omega(\max) = 50$ rad/s. As aforementioned, the mass m, the inertance I_{Iner}, and the damping coefficient ξ_2 are controlling parameters, and we optimize them to achieve assumed goals. Based on equations of the motion (equations (1, 2)) the total inertia of the TMDI is equal to sum of m and I_{Iner}. It allows for designing less massive TMDI than classical TMD because part of active inertia is included in the main system mass. To have

more information about the distribution of the inertia between m and I_{Iner}, we also monitor their ratio:

$$m_{\text{ratio}} = \frac{I_{\text{Iner}} + m}{m}. \tag{3}$$

The optimization algorithm is implemented in Matlab using the function `fmincon`.

We assume two optimization goals:

Minimum of integral of the FRC of main system in range: $[\omega(\min),\ \omega(\max)]$

In the first approach, we optimize the parameters of the system to obtain the minimum area under FRC for the assumed range of the excitation frequency:

$$\min_{\omega\in[\omega(\min),\,\omega(\max)]} \int_{\omega(\min)}^{\omega(\max)} \text{Amp}_x(\omega, I_{\text{Iner}}, \xi_2, m)\,\mathrm{d}\,\omega,$$

thus, we ensure that while varying the excitation frequency the system will follow the minimum path, which directly corresponds to the path with the minimum energy for the whole range.

Minimum of maximum amplitude of the main system in range: $[\omega(\min),\ \omega(\max)]$

In the second approach, we optimize the system parameters to have minimum of the maximum amplitude, hence we just focus on one value along the FRC:

$$\min_{\omega\in[\omega(\min),\,\omega(\max)]} \max(\text{Amp}_x(\omega,\, I_{\text{Iner}},\, \xi_2,\, m)).$$

This optimization procedure corresponds to the classical optimization scheme, which has been derived by Den Hartog. Den Hartog studied the mitigation of undamped main system ($\xi_1 = 0$) and classical TMD (without inerter), hence he could find an analytical condition for minimization of main mass amplitude. In our case, we have to perform numerical optimization. The detection of maximum amplitude along the FRC can be implemented classically, by calculation of the derivative of $\text{Amp}_x(\omega, I_{\text{Iner}}, \xi_2, m)$ and equating it to zero. It gives local extremes, so the one with the highest amplitude is the global maximum. The other option is a numerical solution with the function `fminbnd`, which allows finding the local minimum of the function in the assumed range. To implement it for our purpose we multiply the $\text{Amp}_x(\omega, I_{\text{Iner}}, \xi_2, m)$ by -1, hence now the maximum is minimum. We implemented both approaches and achieved identical results. However, symbolic calculations in Matlab are significantly slower than numerical calculation, so we use the second approach (it is approximately 100 times faster).

4. OPTIMIZATION

This section includes the results of the optimization procedure. It is divided into two separate cases (two goals of optimization). However, to present our results in a clear manner first we do not optimize all selected parameters but we fixed the mass of the TMDI to $m = 11.26$ kg. Then, we extend the analysis for all parameters. It allows us to present the procedure, and the response of the system and better understand the results.

4.1. TMDI with damping coefficient

4.1.1. Minimization of maximum amplitude optimization

Now, we show the optimization procedure that allows us to find the optimal damping coefficient for a given value of inertance I_{Iner} and fixed mass of the TMD $m = 11.26$ kg. In the first step we calculated the response of the system for selected values of $I_{\text{Iner}} \in [1,\ 20]$ kg with step 0.01 kg with varying damping coefficient in range $\xi_2 \in [0.1,\ 0.4]$ with step 0.0001. The results are shown in Fig. 2(a). We plot the amplitude Amp_x versus damping coefficient ξ_2 for different values of I_{Iner}. To have better visibility of the plot, we just show selected lines. Each gray line corresponds to different values of I_{Iner}. The first line is marked with an asterisk for $I_{\text{Iner}} = 1$ kg, then the consecutive lines correspond to an increase of inertance with step equal to 1 kg. The blue line at the bottom of the plot marks the repose of the main system with minimum amplitude Amp_x in the whole considered range of I_{Iner}. The red line connects the minimum of amplitudes in all calculated lines. As it is easy to see, in the beginning, the increase of inertance I_{Iner} causes the decrease of the main system amplitude to some minimum value, and then we observe the increase of the amplitude. Hence, there is the optimum pair of parameters I_{Iner} and ξ_2. At the bottom of the figure is a plateau, where the amplitude hardly changes. The different projection of the red line is shown in panel (b). Now, in the horizontal axis, we have the inertance I_{Iner}, and in the left and right vertical axes, we show the damping coefficient ξ_2 (red line) and the amplitude of the main system Amp_x (green line). The aforementioned plateau is clearly visible close to the minimum amplitude. The optimum values of I_{Iner} and ξ_2 change nearly linearly with respect to I_{Iner}. In panel (c), we show zoom close to minimum value of the amplitude for $I_{\text{Iner}} \in [10.75,\ 10.80]$ kg. Now, we see the response of the system close to the plateau. The optimal parameters are in its middle for $I_{\text{iner}} = 10.7698$ kg, $\xi_2 = 0.194219$, where the amplitude is equal to $\text{Amp}_x = 0.0242$ kg. Moreover, we see that the amplitude of the main system has the same levels before and after the minimum value. In the last panel (d), we show three FRCs for optimal inertance and damping coefficient (black line: $I_{\text{iner}} = 10.7698$ kg, $\xi_2 = 0.194219$), after minimum value of Amp_x (red line: $I_{\text{iner}} = 10.7846$ kg, $\xi_2 = 0.19977$) and before minimum value of Amp_x (green line: $I_{\text{iner}} = 10.7588$ kg, $\xi_2 = 0.189625$). The optimum values have also been calculated in two parameters optimization (varying ξ_2 and I_{Iner}) and we reach the same outcome. As it is easy to see, for optimum value, the amplitude is minimal, and two resonance peaks have the same height, while before this value, the left peak is higher and after the right one. Hence, the minimum amplitude occurs for the same condition as in classical optimization proposed by Den Hartog. The results confirm that the proper selection of the inertance and damping coefficient has a significant influence on the effectiveness of TMDI. From a practical point of view, it is important that the range with the smallest amplitude is not very

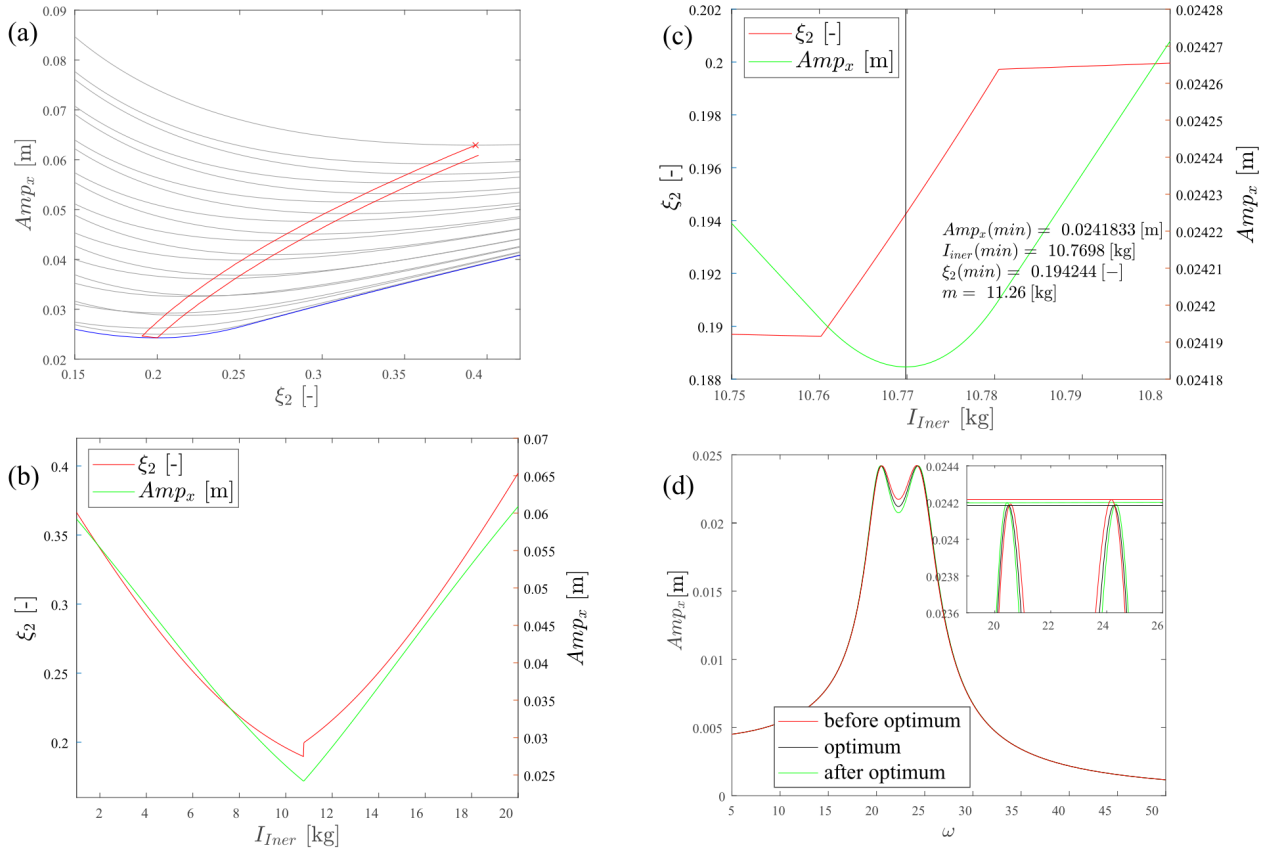

Fig. 2. The minimization of maximum amplitude for $m = 11.26$ kg: (a) the amplitude Amp_x versus damping coefficient ξ_2 for different values of $I_{\mathrm{Iner}} \in [1, 20]$ kg (each gray line corresponds to different values of I_{Iner}, the asterisk marks line for $I_{\mathrm{Iner}} = 1$ kg, other lines are calculated with step 1 kg, blue line marks line with minimum amplitude for whole considered values of I_{Iner}), red line connects the minimum of amplitudes in each line; (b) the optimum values of ξ_2 and corresponding amplitude Amp_x for varying I_{Iner} in range $[1, 20]$ kg with step 0.01 kg; (c) zoom of panel (b) in range $I_{\mathrm{Iner}} \in [10.75, 10.80]$ kg; (d) FRCs for three selected pairs of $(I_{\mathrm{iner}}, \xi_2)$ with six digits precision: $I_{\mathrm{iner}} = 10.7698$ kg, $\xi_2 = 0.194219$ (black line – minimum value of Amp_x), $I_{\mathrm{iner}} = 10.7846$ kg, $\xi_2 = 0.19977$ (green line – after minimum value of Amp_x) and $I_{\mathrm{iner}} = 10.7588$ kg, $\xi_2 = 0.189625$ (red line – before minimum value of Amp_x). In box is magnification of resonances, the horizontal lines show maximum for each case

narrow so that the small mismatches in the system parameters do not strongly affect the properties of the TMDI.

In the next step, we extend the analysis to show the optimization for varying mass m of the TMDI. Hence, we assume mass $m \in [5.0, 30.0]$ kg with step 0.05 kg and for each value of mass m we minimize amplitude Amp_x in respect of two parameters: I_{Iner} and ξ_2. The results are presented in Fig. 3. In panel (a), we show the optimum value of I_{Iner} and ξ_2 for given mass m and corresponding amplitude Amp_x (multiplied 10 times for better visibility). Additionally, we also show the integral under FRC in range $\omega \in [5, 50]$ rad/s. It is visible that with the increase of mass m, the amplitude of the main mass is also decreasing. The inertance is maximum for the smallest mass m, and then it decreases, while for damping coefficient ξ_2 we observe the opposite tendency. Hence, the more massive the TMDI is, the more energy it dissipates from the main mass. However, as it is obvious, it is impossible to add mass to TMDI, and we must restrict the mass m to a reasonable fraction of the mass of the main body. In panel (b) we show the sum of mass m and I_{Iner}: ($m_{\mathrm{sum}} = m + I_{\mathrm{Iner}}$) and ratio between mass m and I_{Iner}: $m_{\mathrm{ratio}} = \dfrac{m - I_{\mathrm{Iner}}}{m}$. The m_{sum} grows with increase of mass m according to quadratic function but it is close to linear function ($m_{\mathrm{sum}} = 18.51 + 0.2473m + 0.005972m^2$). The m_{ratio} gives us information when mass m becomes larger than inertance I_{Iner}. It occurs for $m = 10.96$ kg. In the beginning, the ratio is growing rapidly, but for larger masses, it tends to a horizontal line because $I_{\mathrm{Iner}} \to 0.0$ kg. In panels (c–h) we show similar plots as in Fig. 2(b,c) for selected mass $m = (5, 10, 15, 20, 25, 30)$ kg to show how the minimum for each mass is approached. We can see that with an increase of mass m, the transition around minimum values is less steep and spans a wider range of I_{Iner}.

4.1.2. Integral optimization

In this optimization strategy, we perform a similar study as in the previous case. Hence, we find the optimal damping coefficient ξ_2 for the given value of inertance I_{Iner} and fixed mass of the TMD $m = 11.26$ kg. In the first step we calculated the response of the system for selected values of $I_{\mathrm{Iner}} \in [1, 16]$ kg with step 0.01 kg with varying damping coefficient in

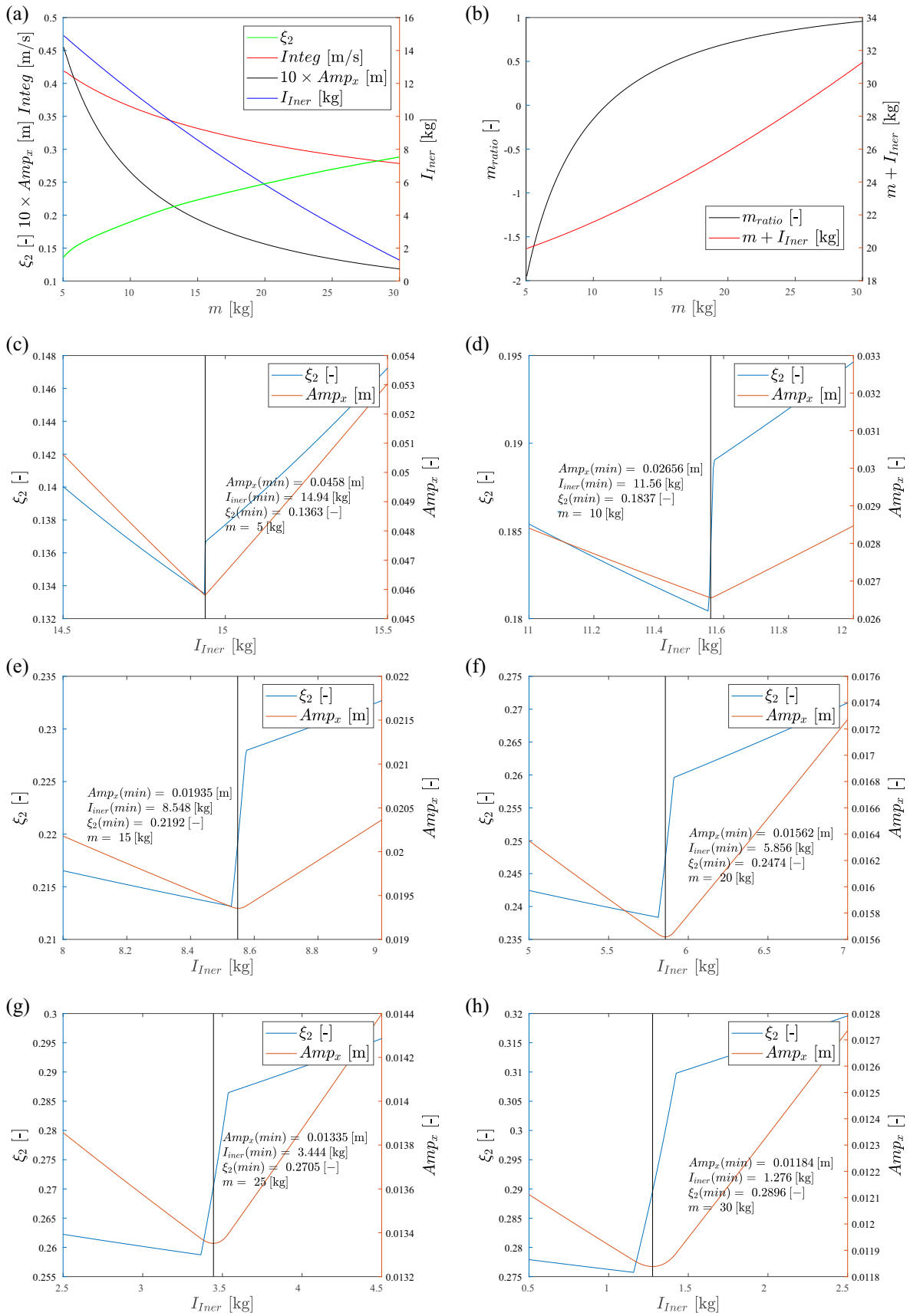

Fig. 3. (a,b) The minimization of amplitude for varying mass m in range $m \in [5.0, 30.0]$ kg with step 0.05 kg: (a) optimum values of I_{iner} and ξ_2 with corresponding values of Amp_x and $Integ$; (b) the m_{ratio} and sum $m + I_{\text{Iner}}$ versus mass m of the TMDI; (c–h) the optimum values of ξ_2 and corresponding amplitude Amp_x for varying I_{Iner} in range $[1, 20]$ kg with step 0.02 kg for $m = [5, 10, 15, 20, 25, 30]$

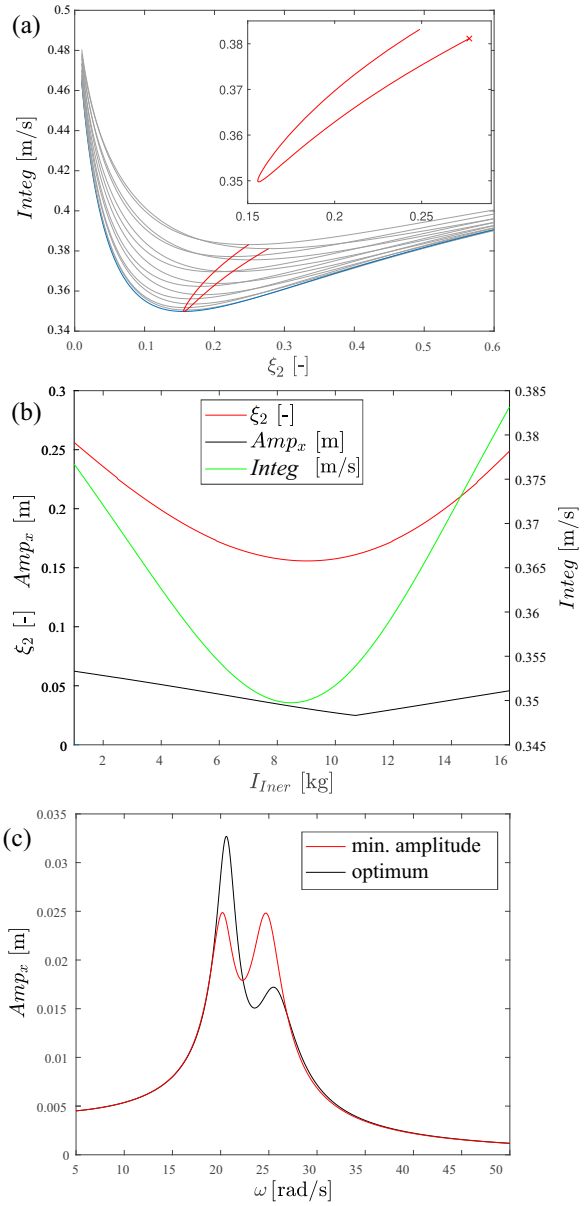

Fig. 4. The minimization of integral for $m = 11.26$ kg: (a) the integral *Integ* versus damping coefficient ξ_2 for different values of $I_{\text{Iner}} \in [1, 16]$ kg (each gray line corresponds to different values of I_{Iner}, the asterisk marks line for $I_{\text{Iner}} = 1$ kg, other lines are calculated with step 1 kg, blue line marks line with minimum amplitude for whole considered values of I_{Iner}), red line connects the minimum of amplitudes in each line; (b) the optimum values of ξ_2, corresponding amplitude Amp_x and *Integ* for varying I_{Iner} in range $[1, 16]$ kg with step 0.01 kg; (c) FRC plots for minimum value of *Integ* (black line) and minimum value of Amp_x (red line).

range $\xi_2 \in [0.1, 0.4]$ with step 0.0001. The results are shown in Fig. 4a. We plot the integral of the FRC *Integ* versus the damping coefficient ξ_2 for different values of I_{Iner}. Each gray line corresponds to different values of I_{Iner} (we plotted just the selected line for better visibility). The first line is marked with an asterisk for $I_{\text{Iner}} = 1$ kg, then the consecutive lines correspond to increase of inertance with step equal to 1 kg. The blue line at the bottom of the plot marks the repose of the main system with the minimum integral of the FRC *Integ* in the whole considered range of I_{Iner}. The red line connects the minimum of amplitudes in all calculated lines. In this case of optimization goal, the line is smooth, and we do not observe any jumps along it. The optimum pair of parameters is as follows: $I_{\text{Iner}} = 8.475$ kg, $\xi_2 = 0.1563$ and corresponding value of system amplitude is $\text{Amp}_x = 0.0327$ m. The optimum values have also been calculated in two parameters optimization (varying ξ_2 and I_{Iner}), and we reach the same outcome. In panel (b), we show the plots of damping coefficient ξ_2, integral of the FRC *Integ* and amplitude of system Amp_x versus inertance I_{Iner}. Now, we can easily see the minimum value along *Integ* line. However, for the minimum value of *Integ*, the amplitude is not minimal. It reaches its minimum ($\text{Amp}_x = 0.02488$ m) for $I_{\text{Iner}} = 10.68$ kg and $\xi_2 = 0.1609$. It is very close to values calculated in optimization based on minimum values of the system amplitude. The Den Hartog condition is, of course, not fulfilled as presented in panel (c), where we show the FRC for optimal values of parameters (black line). We additionally present the response for the minimum value of amplitude, which is close to the Den Hartog condition.

Then, we present the optimization for varying mass m of the TMDI. Hence, we assume that mass is varying in range $m \in [5.0, 30.0]$ kg with step 0.05 kg and for each value of mass m, we minimize the integral of the FRC *Integ* in respect of two parameters: I_{Iner} and ξ_2. The results are presented in Fig. 5. In panel (a), we show the optimum value of I_{Iner} and ξ_2 for given mass m and corresponding integral under FRC in range

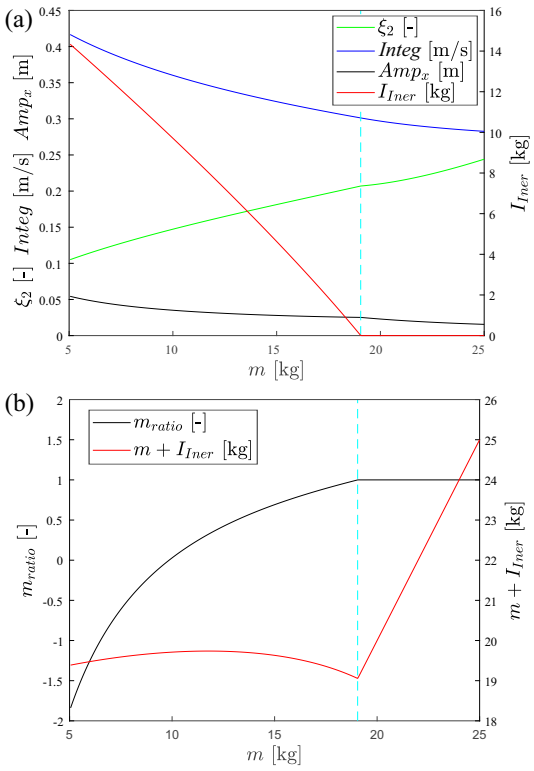

Fig. 5. The minimization of integral for varying mass m in range $m \in [5.0, 30.0]$ kg with step 0.05 kg: (a) optimum values of I_{iner} and ξ_2 with corresponding values of I_{iner} and Amp_x; (b) the m_{ratio} and sum $m + I_{\text{Iner}}$ versus mass m of the TMDI

$\omega \in [5, 50]$ rad/s. Additionally, we also show the amplitude Amp_x. In panel (b) we present the m_{ratio} and sum $m_{\mathrm{sum}} = m + I_{\mathrm{Iner}}$ versus mass of the TMDI. In both plots, we can see a significant difference compared to the first optimization goal. For $m = 19.05$ kg the I_{Iner} reaches zero and it persists with this value with further increase of mass m. Thus, for the mass of TMDI above this threshold, in the case of integral minimization, the system is reduced to classical TMD. However, one has to take into account that the ratio between the main mass ($M = 102.66$ kg) and TMD mass m is high, and in most applications, it is impossible to use such a massive TMD. Below the bound value, we observe a similar tendency as for the first type of optimization. The more mass m, the more decrease of integral $Integ$ and amplitude Amp_x of TMDI we observe. However, the difference is visible in panel (b), where for $m < 19.05$ kg the sum of $m_{\mathrm{sum}} = m + I_{\mathrm{Iner}}$ is nearly constant with mean value 19.57 kg and standard deviation 0.166. It means that the best damping properties of TMDI, considering the integral condition, are for a similar sum of inertia and mass of the TMDI. In engineering practice, it is necessary to decide which mass m and/or integral is acceptable for the system and design the TMDI based on selected assumption.

5. CONCLUSIONS

In this paper, we present the optimization of the TMDI. The optimization scheme is based on the analytical solution of linear ordinary differential equations. The goal is to find the optimum parameters of TMDI, namely, the mass of the body, damping coefficient, and inertance. We tune parameters based on two schemes. The first one is the minimization of the amplitude of the damped system, while the second one minimizes the overall response under the FRC. The results show that selecting proper values of all parameters of TMDI is crucial for achieving the significant mitigation of the damped system oscillations. The important factor is the relation between mass and inertance. We show that for the TMDI with a small mass and large inertance, the response is significantly larger than for the TMDI with a large mass and small inertance. However, the TMDI with a large mass is usually not applicable because it is too massive with respect to the total mass of the system. Summarizing, the presented results give an overview of possible tuning schemes of the TMDI parameters for the different masses of the TMDI and allow us to find the optimal parameter values of the mitigating system.

ACKNOWLEDGEMENTS

This work has been supported by National Science Centre, Poland - Project No. 2015/17/B/ST8/03325.

REFERENCES

[1] M. Abe, "Semi-active tuned mass dampers for seismic protection of civil structures," *Earthq. Eng. Struct. Dyn.*, vol. 25, no. 7, pp. 743–749, 1996.

[2] A. Andersson, A. O'Connor, and R. Karoumi, "Passive and adaptive damping systems for vibration mitigation and increased fatigue service life of a tied arch railway bridge," *Comput.-Aided Civil Infrastruct. Eng.*, vol. 30, no. 9, pp. 748–757, 2015.

[3] T. Pinkaew and Y. Fujino, "Effectiveness of semi-active tuned mass dampers under harmonic excitation," *Eng. Struct.*, vol. 23, no. 7, pp. 850–856, 2001.

[4] M. Setareh, "Application of semi-active tuned mass dampers to base-excited systems," *Earthq. Eng. Struct. Dyn.*, vol. 30, no. 3, pp. 449–462, 2001.

[5] P. Brzeski, T. Kapitaniak, and P. Perlikowski, "Novel type of tuned mass damper with inerter which enables changes of inertance," *J. Sound Vib.*, vol. 349, pp. 56–66, 2015.

[6] P. Brzeski, M. Lazarek, and P. Perlikowski, "Experimental study of the novel tuned mass damper with inerter which enables changes of inertance," *J. Sound Vib.*, vol. 404, pp. 47–57, 2017.

[7] Y. Hu, M.Z. Chen, S. Xu, and Y. Liu, "Semiactive inerter and its application in adaptive tuned vibration absorbers," *IEEE Trans. Control Syst. Technol.*, vol. 25, no. 1, pp. 294–300, 2016.

[8] W. Shi, L. Wang, and Z. Lu, "Study on self-adjustable tuned mass damper with variable mass," *Struct. Control Health Monitor.*, vol. 25, no. 3, p. e2114, 2018.

[9] W. Shi, L. Wang, Z. Lu, and H. Wang, "Experimental and numerical study on adaptive-passive variable mass tuned mass damper," *J. Sound Vib.*, vol. 452, pp. 97–111, 2019.

[10] G.-L. Lin, C.-C. Lin, B.-C. Chen, and T.-T. Soong, "Vibration control performance of tuned mass dampers with resettable variable stiffness," *Eng. Struct.*, vol. 83, pp. 187–197, 2015.

[11] C. Sun and S. Nagarajaiah, "Study on semi-active tuned mass damper with variable damping and stiffness under seismic excitations," *Struct. Control Health Monitor*, vol. 21, no. 6, pp. 890–906, 2014.

[12] P. Walsh and J. Lamancusa, "A variable stiffness vibration absorber for minimization of transient vibrations," *J. Sound Vib.*, vol. 158, no. 2, pp. 195–211, 1992.

[13] D.H. Wang and W.H. Liao, "Magnetorheological fluid dampers: a review of parametric modelling," *Smart Mater. Struct.*, vol. 20, no. 2, p. 023001, jan 2011.

[14] N. Varadarajan and S. Nagarajaiah, "Wind response control of building with variable stiffness tuned mass damper using empirical mode decomposition/hilbert transform," *J. Eng. Mech.*, vol. 130, no. 4, pp. 451–458, 2004.

[15] F. Weber and M. Maślanka, "Frequency and damping adaptation of a tmd with controlled mr damper," *Smart Mater. Struct.*, vol. 21, no. 5, p. 055011, 2012.

[16] K. Mnich, M. Lazarek, P. Brzeski, and P. Perlikowski, "Experimental investigation and modeling of nonlinear, adaptive dashpot," *Meccanica*, vol. 55, no. 12, pp. 2599–2608, 2020.

[17] D. Hartog, *Mechanical vibrations*, 5th ed. Dover Publications, inc., 1985, ch. 3, pp. 93–100.

[18] T. Asami, O. Nishihara, and A.M. Baz, "Analytical Solutions to H∞ and H2 Optimization of Dynamic Vibration Absorbers Attached to Damped Linear Systems ," *J. Vib. Acoust.*, vol. 124, no. 2, pp. 284–295, 03 2002.

[19] A. Ghosh and B. Basu, "A closed-form optimal tuning criterion for tmd in damped structures," *Struct. Control Health Monitor.*, vol. 14, no. 4, pp. 681–692, 2007.

[20] G.C. Marano, R. Greco, and B. Chiaia, "A comparison between different optimization criteria for tuned mass dampers design," *J. Sound Vib.*, vol. 329, no. 23, pp. 4880–4890, 2010.

[21] N. Hoang, Y. Fujino, and P. Warnitchai, "Optimal tuned mass damper for seismic applications and practical design formulas," *Eng. Struct.*, vol. 30, no. 3, pp. 707–715, 2008.

[22] P. Brzeski and P. Perlikowski, "Effects of play and inerter nonlinearities on the performance of tuned mass damper," *Nonlinear Dyn.*, vol. 88, no. 2, pp. 1027–1041, 2017.

[23] L. Marian and A. Giaralis, "The tuned mass-damper-inerter for harmonic vibrations suppression, attached mass reduction, and energy harvesting," *Smart Struct. Syst.*, vol. 19, no. 6, pp. 665–678, 2017.

[24] Y. Wang, H.-X. Li, H.-D. Meng, and Y. Wang, "Dynamic characteristics of underframe semi-active inerter-based suspended device for high-speed train based on lqr control," *Bull. Pol. Acad. Sci. Tech. Sci.*, vol. 70, no. 4, p. e141722, 2022.

[25] P. Brzeski, M. Lazarek, and P. Perlikowski, "Influence of variable damping coefficient on efficiency of tmd with inerter," *Energies*, vol. 13, no. 23, p. 6175, 2020.